BBA - Molecular Basis of Disease 1867 (2021) 166155

Contents lists available at ScienceDirect

BBA - Molecular Basis of Disease

journal homepage: www.elsevier.com/locate/bbadis

TLR4 expression and functionality are downregulated in glioblastoma cells and in tumor-associated macrophages: A new mechanism of immune evasion?

L.L.P. da Cruz [a], P.O. de Souza [b], M. Dal Prá [b], M. Falchetti [c], A.M. de Abreu [b], J.H. Azambuja [b], A. P.S. Bertoni [a], A.H.R. Paz [d], A.B. Araújo [e], F. Visioli [f], T. Fazolo [g], G.G. da Silva [h], P.V. Worm [h,i], M. R. Wink [a,b], A. Zanotto-Filho [c], E. Braganhol [a,b,j,*]

[a] Programa de Pós-Graduação em Ciências da Saúde, Universidade Federal de Ciências da Saúde de Porto Alegre (UFCSPA), Porto Alegre, RS, Brazil
[b] Programa de Pós-Graduação em Biociências, UFCSPA, Porto Alegre, RS, Brazil
[c] Programa de Pós-Graduação em Farmacologia, Universidade Federal de Santa Catarina (UFSC), Florianópolis, SC, Brazil
[d] Departamento de Morfologia, Universidade Federal do Rio Grande do Sul (UFRGS), Porto Alegre, RS, Brazil
[e] Centro de Processamento Celular, Hospital de Clínicas de Porto Alegre (HCPA), Porto Alegre, RS, Brazil
[f] Faculdade de Odontologia, UFRGS, Porto Alegre, RS, Brazil
[g] Hospital Moinhos de Vento, Porto Alegre, RS, Brazil
[h] Hospital São José, Irmandade Santa Casa de Misericórdia de Porto Alegre (ISCMPA), Porto Alegre, RS, Brazil
[i] Departamento de Cirurgia, UFCSPA, Porto Alegre, RS, Brazil
[j] Instituto de Cardiologia do Rio Grande do Sul/Fundação Universitária do Instituto de Cardiologia (IC-FUC), Porto Alegre, RS, Brazil

ARTICLE INFO

Keywords:
TLR4
Glioblastoma
Chemoresistance
Macrophages
Immune evasion

ABSTRACT

Glioblastoma (GB) is the most common and aggressive form of primary brain tumor, in which the presence of an inflammatory environment, composed mainly by tumor-associated macrophages (TAMs), is related to its progression and development of chemoresistance. Toll-Like Receptors (TLRs) are key components of the innate immune system and their expression in both tumor and immune-associated cells may impact the cell communication in the tumor microenvironment (TME), further modeling cancer growth and response to therapy. Here, we investigated the participation of TLR4-mediated signaling as a mechanism of induced-immune escape in GB. Initially, bioinformatics analysis of public datasets revealed that TLR4 expression is lower in GB tumors when compared to astrocytomas (AST), and in a subset of TAMs. Further, we confirmed that TLR4 expression is downregulated in chemoresistant GB, as well as in macrophages co-cultured with GB cells. Additionally, TLR4 function is impaired in those cells even following stimulation with LPS, an agonist of TLR4. Finally, experiments performed in a cohort of clinical primary and metastatic brain tumors indicated that the immunostaining of TLR4 and CD45 are inversely proportional, and confirmed the low TLR4 expression in GBs. Interestingly, the cytoplasmic/nuclear pattern of TLR4 staining in cancer tissues suggests additional roles of this receptor in carcinogenesis. Overall, our data suggest the downregulation of TLR4 expression and activity as a strategy for GB-associated immune escape. Additional studies are necessary to better understand TLR4 signaling in TME in order to improve the benefits of immunotherapy based on TLR signaling.

1. Introduction

Glioblastoma (GB) is the most common and aggressive form of primary brain tumor [1,2]. Despite intense efforts, patient prognosis remains dismal (12–18 months). The success of therapy is limited by the development of chemoresistance and by the presence of an inflammatory microenvironment, which is fundamental for GB progression [3–7].

Although the mechanisms correlating innate immunity, inflammation, and cancer are unclear, studies have shown that Toll-Like Receptors (TLRs) are expressed by both tumor and immune cells, thereby

* Corresponding author at: Universidade Federal de Ciências da Saúde (UFCSPA), Sarmento Leite St, 245 – Main Building – Room 304, 90.050-170 Porto Alegre, RS, Brazil.
E-mail address: ebraganhol@ufcspa.edu.br (E. Braganhol).

https://doi.org/10.1016/j.bbadis.2021.166155
Received 12 October 2020; Received in revised form 30 March 2021; Accepted 22 April 2021
Available online 28 April 2021

impacting the cell communication in the tumor microenvironment (TME) [8]. TLRs are components of the innate immune response that recognize and respond to both pathogen-associated molecular patterns (PAMPs) and damage-associated molecular patterns (DAMPs), which consist of exogenous and endogenous ligands, respectively [9,10]. DAMPs could be chronically released as a result of chemo/radiotherapy triggering an aseptic inflammatory response, which may further impact cancer progression [8,11].

The expression of TLRs has been reported in a variety of tumors, including hepatocellular carcinoma, colorectal, prostate, and bladder cancer [12], and is frequently associated with disease prognosis [10]. However, the precise result of TLR signaling in cancer remains a challenge [13]. For example, the anti-tumorigenic role of TLRs is associated to their stimulation by PAMPs/DAMPs on immature antigen-presenting cells (APCs), resulting in a specific cancer cytotoxic response [14–16]. Based on this principle, many clinical trials using TLRs agonists were performed, exhibiting varied efficiency that remains to be defined [17,18]. On the other hand, TLRs sensitization may mediate a chronic inflammatory response, which is a hallmark of cancer. Indeed, TLR4 overexpression is generally associated with IL-6 and IL1β production, which favor tumor maintenance [10,19,20]. In GB, the low TLR4 expression in self-renewing cancer stem cells (CSC) is related to stemness maintenance, allowing those cells to survive by disregarding immune signaling [21]. As different populations of cells express TLRs, which are differentially stimulated by PAMPs/DAMPs, the dual role of TLR signaling in TME may be expected and need to be better understood.

Therefore, considering that an inflammatory microenvironment rich in tumor-associated macrophages (TAMs) has a key role on GB progression, and the dual activity of TLR signaling in cancer progression, here we investigated the participation of TLR signaling in the scenario of GB chemoresistance. *In silico* analysis and TLR4 expression were investigated in human tumor specimens and in TAM. The expression and functionality of TLR4 was assessed in TMZ-sensitive and TMZ-resistant GB cells, and in macrophages co-cultured with GB cells. This study may provide insights about the participation of TLR4 signaling in the immune-tumor cell interaction, enabling the development of an efficient immunotherapy against GB.

2. Material and methods

2.1. Materials

Chemicals applied in the present study were described in Supplementary Table 1. All other chemicals and solvents were obtained from standard commercial suppliers with analytical grade and were used as received.

2.2. Bioinformatics analysis

2.2.1. Datasets

Gene expression profiling across glioma histological subtypes and non-tumor specimens were evaluated in GSE68848 (Rembrandt cohort; $n = 580$ samples), GSE16011 ($n = 284$ samples) and GSE4290 (Henry Ford Hospital cohort; $n = 180$ samples) datasets. Microarray data were generated from Affymetrix U133 Plus 2.0 microarray platform, and downloaded from the Gene Expression Omnibus. The datasets were imported into R analysis environment by using the *GEOquery package*. Expression data was annotated and normalized. Genes were annotated with the *hgu133plus2.db package*, and expression data was quantile normalized using the *affyPLM* package. Only samples annotated as "astrocytoma" (AST) and "oligodendroglioma" (ODG), "glioblastoma" (GB), and "non-tumor/normal" (NT) were analyzed. In case of multiple probes to the same gene, the summarization was carried out by calculating the gene mean value. Differential expression of TLR4 and CD14 in microarrays was evaluated by empirical Bayes statistics available in the *limma* package, and an adjusted *p*-value <0.05 was considered statistically significant. For the single-cell analysis, the GSE84465 dataset [22] comprising $n = 3589$ single-cell RNA-sequencing from tumor core and peritumoral regions of 4 GBM specimens/patients was evaluated. Single cell comprised RNA sequencing and phenotyping of myeloid ($CD45^+$), astrocytes ($HepaCAM^+$), neoplastic/GBM, vascular endothelial (BSL-1), oligodendrocyte progenitor cells, neurons ($CD90^+$) and oligodendrocytes (anti-O4 $hybridoma^+$). Gene counts, cell type phenotyping and 2D-tSNE (t-distributed stochastic neighbor embedding) representation of included cells were downloaded from http://gbmseq.org/. Gene expression data were log2 transformed, and genes with zero counts per million (CPM) in all cells were excluded. We further separated the $CD45^+$ cell subset into macrophages and microglia by using the following markers: microglia (*ADORA3*, *GPR34*, *OLFML3*, *P2RY12*, *SALL1*, *SLC2A5*, *TMEM119*); macrophage (*ANXA1*, *CRIP1*, *EMILIN2*, *S100A8*, *S100A9*) [22,23]. Only $CD45^+$ sorted cells with detectable RNA sequencing counts (log2 CPM > 0) for the CD45/*PTPRC* gene were used. $CD45^+$ cells were clustered with the *pheatmap* package using Euclidean distances and *Ward.D2* clustering methods.

2.2.2. Gene set signature expression

In order to estimate the enrichment scores for M1, M2 and TAM macrophages, gene sets representative of M1-like (*CCL2*, *CCL3*, *CCL5*, *CCR7*, *CD38*, *CD40*, *CD80*, *CD86*, *CXCL10*, *CXCL11*, *CXCL16*, *CXCL9*, *FCGR1A*, *FCGR2A*, *HLA-DRA*, *IDO1*, *IFNG*, *IL12A*, *IL12B*, *IL15*, *IL18*, *IL1A*, *IL1B*, *IL1R1*, *IL23A*, *IL6*, *IRF5*, *KYNU*, *NOS2*, *SIGLEC1*, *STAT1*, *TNF*, *TLR2 and TLR4*), M2-like (*CCL16*, *CCL17*, *CCL18*, *CCL22*, *CCL24*, *CD163*, *CD200R1*, *MRC1*, *MSR1*, *FCER2*, *EGF*, *FGF2*, *IL10*, *IL1RN*, *LTA*, *CLEC7A*, *CLEC10A*, *TGFB1*, *TGM2*, *VEGFA*, *MARCO*, *CD209*, *IRF4*, *SOCS1*, *GATA3*, *STAB1*, *MMP1*, *MMP12*, *TGFBR2*) and Tumor-Associated Macrophages (TAM) (*ADGRE2*, *ANGPT1*, *ANGPT2*, *C1QA*, *C1QB*, *C1QC*, *CCL17*, *CCL18*, *CCL2*, *CCL22*, *CCL3*, *CCR2*, *CD163*, *CD68*, *CD74*, *CHI3L1*, *CLEC10A*, *CLEC7A*, *CSF1*, *CSF1R*, *CTGF*, *CX3CR1*, *CXCR4*, *EGF*, *EGFR*, *FCER2*, *FCGR2A*, *FCGR3A*, *FGF2*, *FLT1*, *HGF*, *HLA-DRA*, *IL10*, *KDR*, *MARCO*, *MMP2*, *MMP9*, *MRC1*, *MSR1*, *PDGFA*, *PECAM1*, *PTGS2*, *STAT3*, *TGFBR2*, *TNF*, *VEGFA*, *VEGFC*) were evaluated from glioma gene expression datasets. These genes were curated from prior studies on GB and on macrophage polarization [24–31]; note that some M1 and M2 genes appear in the TAM gene set, given that TAM can express both M1 and M2 markers, depending on tumor stage and microenvironment/region. For estimating signature expression scores, normalized expression values of each gene "i" for sample "j" were transformed to *Z*-score values (Zij) with mean $\mu = 0$ over all samples/row. M1/M2/TAM signature score per sample was calculated by summing the Z-scores of each in-signature gene with a sample, and then normalized into a combined Z-score across all samples [32]. Signature scores per sample were then pooled into their respective phenotypes (*i.e.* GB, AST, ODG and NT) and plotted. Thus, for a signature to be up/downregulated, a significant number of genes are required to change expression in the same direction.

2.3. General cell culture procedures

2.3.1. Glioma cell line cultures and chemoresistance induction protocol

Mouse GL261 (isogenic to C57/BL-6 mice) and human U87MG glioma cell lines were obtained from ATCC (American Type Cell Collection; Rockville, Maryland, USA). Cells were grown in culture flasks and maintained in Dulbecco's modified Eagle's medium (DMEM) (pH 7.4) containing 8.4 mM HEPES, 23.8 mM sodium bicarbonate ($NaHCO_3$), 0.1% fungizone, 100 U/L penicillin/streptomycin 0.5 U/mL, and supplemented with 10% (v/v) FBS. Cells were incubated at a temperature of 37 °C, a minimum relative humidity of 95%, and a 5% CO_2 atmosphere. Chemoresistance phenotype was induced in GL261 and U87MG by exposing glioma cells to increasing TMZ concentrations (2.5–2500 μM and 2.5–320 μM for GL261 and U87MG, respectively) for a period of 4 to 6 months [33,34]. For maintenance of chemoresistance phenotype, GLTMZ and U87TMZ cells were cultivated in DMEM/10% FBS as

described above in the presence of TMZ (160 μM).

2.3.2. Primary mouse and human macrophage cultures and co-cultures with glioblastoma cells

Peritoneal macrophages from mouse male C57BL/6 (6–8 weeks) were collected by lavage of peritoneal cavity with DMEM/FBS-free medium as previously described [34]. Briefly, cells were centrifuged and suspended in DMEM/FBS-free medium, and the obtained cells were seeded in 6 multi-well plates (1×10^6 cells/well). Macrophages were allowed to attach for 30 min. Then, the medium containing unattached cells was removed and the mouse macrophages were directly co-cultured with GL or GLTMZ (6×10^4 cells/well).

Primary human macrophages were obtained from differentiation of circulating monocytes as previously described [35,36] with minor modifications. Briefly, monocytes were isolated from total blood of umbilical cord using Histopaque®-1077 density gradient; cells were seeded in 6 multi-well plates (7×10^6 cells/well) and differentiated into macrophages by stimulation with GM-CSF (50 ng/mL) for 7 days. Subsequently, mature human macrophages were directly co-cultured with U87 or U87TMZ (6×10^3 cells/well). The analyses were performed 18 h following glioma-macrophage co-cultures. GL, GLTMZ, U87 or U87TMZ glioma cells or mouse/human macrophages cultured in DMEM/10% FBS under the same conditions were considered controls. All procedures used in the present study followed the Principles of Care from NIH and were approved by the Ethical Committee of UFCSPA (protocol number 157/14) or by the Ethical Committee of Hospital de Clínicas de Porto Alegre (protocol number 2.476.898) for experiments performed in mice or with human blood, respectively.

2.4. Cell proliferation and viability assays

2.4.1. Cell counting assay

For cell proliferation analysis, GL and GLTMZ were seeded in 24 well plates (1×10^4 cells/well) in DMEM/10% FBS and cells were allowed to grow for 48 h. Subsequently, the culture medium was replaced by fresh DMEM/0.5% FBS, and after 24 h glioma cells were treated with LPS (100 ng/mL) or HMGB1 (1 μg/mL) in DMEM/0.5% FBS. In experiments using TLR4 antagonist, Sparstolonin B (SsnB; 10 or 100 μM) was added to the culture 30 min before LPS [37]. Cell number was assessed 18 h later by cell counting using a hemocytometer. Glioma cells exposed to DMEM/0.5% FBS or to DMEM/10% FBS were considered negative and positive controls of cell proliferation, respectively. Data were expressed as cell number per well.

2.4.2. MTT assay

GL and GLTMZ glioma cells were seeded in 96 well plates (10×10^3 cells/well) in DMEM/10% FBS and cell viability was determined after 48 or 72 h of culture by soluble MTT reduction assay [3-(4,5-dimethylthiazol-2-yl)-2,5-diphenyltetrazolium bromide] to formazan crystals as previously described [38]. The absorbance was determined at 492 nm on a microplate reader (SpectraMax® M3– Molecular Devices). Data were expressed as absorbance.

2.4.3. BrdU assay

GL or GLTMZ cell lines were seeded in 6 well plates (6×10^4 cells/well) in DMEM/10% FBS. For DNA synthesis analysis, the culture medium (DMEM/10% FBS) was replaced by fresh DMEM/0.5% FBS. After 22 h of starvation, cells were exposed to 10 μM bromodeoxyuridine (BrdU) for 2 h incubation in DMEM/10% FBS. Cells were then incubated with anti-BrdU-PE antibody (1:50 dilution; BD Biosciences) and the percentage of BrdU-incorporating cells was determined by flow cytometry (FACSCanto II Flow Cytometer; BD Biosciences).

2.5. Cell migration assay

GL and GLTMZ glioma cells were seeded in 12 well plates (5×10^4 cells/well). The wound healing assay was carried out as described previously [39]. Briefly, a pipette-200 tip was used to create a lesion in the cell monolayer to generate the "wound". GL and GLTMZ cell cultures were washed with PBS to remove debris and cells were treated with LPS (1, 10 and 100 ng/mL) or HMGB1 (1 μg/mL) in DMEM/0.5% FBS. Closure of the wound was monitored in an inverted microscope (40×) at time intervals of 0, 6, 12 and 24 h after scratching the monolayer. Cells exposed to DMEM/0.5% FBS and DMEM/10% FBS were considered negative and positive controls of migration. Quantitative analysis of the cell-free slit was performed using ImageJ software (National Institutes of Health, USA) and the cell migration was expressed in percentage.

2.6. Quantitative real-time PCR analysis

Total RNA was isolated from the cells using Trizol (Invitrogen) according to the manufacturer's instructions and quantified by spectrophotometry at 260 nm. One microgram of RNA was reverse-transcribed to cDNA using Superscript III reverse transcriptase kit (Invitrogen) following the manufacturer's instructions. qPCR was carried out in the Applied-Biosystems Step One Plus cycler using Fast SYBR Green Master Mix (Applied Biosystems) following the manufacturer's instructions. Sequences of TLR and constitutive gene primers are listed in Supplementary Table 2. As a control for genomic DNA contaminations of the RNA preparation, PCR reactions were also performed in the absence of reverse-transcription, and no signal was detected in these samples. All results were analyzed in relation to a standard curve generated with sequential dilutions (10× to 100×) of a pooled cDNA sample. TBP [40] and Ppia (Table 3S) expression were used as internal control genes for human and mouse expression calculations, as determined by NormFinder® software [41].

2.7. Determination of CD11b expression, active TLR4/MD2 complex and cytokine production by flow cytometry

Primary mouse peritoneal macrophages co-cultured with GL or GLTMZ were obtained as described above (Section 2.2.2). Cultures in either absence or presence of LPS stimulation (100 ng/mL for 24 h) were washed with PBS and carefully detached with cold EDTA solution (2.5 μM) using a cell scraper. The cell viability of detached cells was determined by cell counting using trypan-blue staining. Samples were then incubated with TLR4/MD2 (1:25; BD Biosciences) and CD11b monoclonal Antibody (M1/70), eFluor 660 (1:160; eBioscience). Primary mouse macrophages, GL and GLTMZ cultured alone, in presence or absence of LPS were considered controls. Results were expressed as the percentage of positive cells. Cytokines (IL-6, IL-10, MCP-1, IFNγ, TNF and IL12p-70) were determined in the supernatant of cell cultures using Cytometric Bead Array (CBA). All analyses were performed by flow cytometry (FACSCanto II Flow Cytometer; BD Biosciences) following the manufacturer's instructions.

2.8. Immunofluorescence analysis

Primary human macrophages co-cultured with U87 or U87TMZ were obtained as described above (Section 2.3.2). Cell cultures were fixed in 10% phosphate-buffered formalin/acetone and sections were incubated for 90 min at RT with the primary mouse monoclonal anti-TLR4 antibody (1:50; SC). They were then incubated with FITC-conjugated anti-mouse antibody (1:1000) for 60 min at RT. Sections were counterstained with DAPI blue (1:10,000). Images were captured using a digital camera connected to a microscope (Olympus, Japan).

2.9. Immunohistochemistry analysis

Human specimens resected from patients with primary ($N = 8$) or metastatic ($N = 2$) brain tumors who underwent operations at Santa Casa de Misericórdia de Porto Alegre (ISCMPA) in 2019. This study was

approved by the institutional review board of UFCSPA, ISCMPA and Commission of Ethic in Research (CEP; protocol number 78664117.0.0000.5345). Informed written consent was obtained from all patients. Two pathologists provided the histological diagnoses according to the revised World Health Organization classification. For immunohistochemistry analysis, paraffin-embedded specimens were cut into 4 μm sections. After deparaffinization with xylol and rehydration, antigen retrieval was performed. Endogenous peroxidase activity was blocked with 3% H_2O_2 in methanol. Primary antibodies against TLR4 (1:100; SC), and CD45 (1:100; DAKO) were used. The immunohistochemical results were evaluated by a pathologist in a blinded manner. Samples were imaged under a DM6B light microscope (Leica Optical).

2.10. Statistical analysis

Data were expressed as mean ± S.D. of at least 3 independent experiments and were subjected to one-way analysis of variance (ANOVA) followed by either Tukey–Kramer *post-hoc* test (for multiple comparisons), Bonferroni test, or Student's *t*-test as appropriate. Differences between mean values were considered significant when $P < 0.05$. For bioinformatics experiments, statistical analysis was performed by Kruskal-Wallis followed by Dunn's *post hoc* tests at a $p < 0.05$ threshold.

3. Results

3.1. TLR4 expression is downregulated in TAM and human GB

The GB microenvironment consists of neoplastic and non-neoplastic cells, with TAMs comprising the majority of infiltrated GB-immune cells [6,7]. Indeed, TAMs constitute up to 40% of tumor bulk, and the important role of TLR4 in the macrophages/microglial immune/inflammatory activities is well established [9,10]. Therefore, we investigated the TLR4 expression in brain tumor cells and in TAMs by *in silico* analysis. We first observed that GB and non-tumor specimens showed

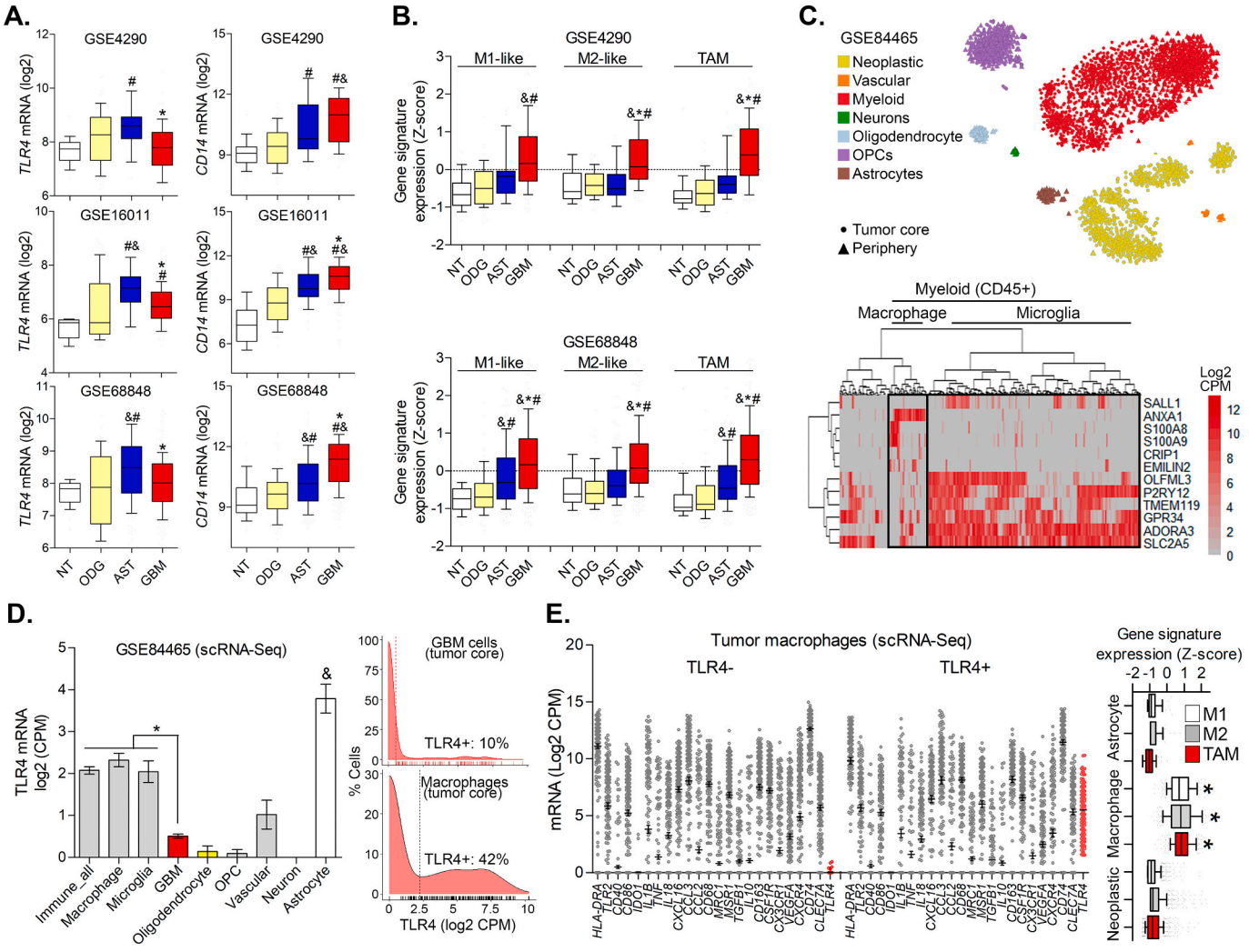

Fig. 1. Analysis of TLR4 expression in brain tumors and in TAM. (A) TLR4 and CD14 expression and (B) M1-, M2- and TAM-like signature expression scores across gliomas histological subtypes (Glioblastoma/GBM, astrocytoma/AST and oligodendroglioma/ODG; TAM - tumor-associated macrophages) from microarray datasets. (C) 2D-tSNE representation of the single cells included in the study (graph generated in http://gbmseq.org/), and heatmap representation of macrophages and microglia clustering of CD45+ cells from GSE84465 dataset [22]. (D) TLR4 mRNA expression across different cell types isolated from GB tumor core (immune/macrophage/microglia, GBM/neoplastic and oligodendrocyte) and tumor periphery (astrocytes and neurons), and histogram representation of TLR4 expression distribution in tumor core neoplastic/GBM cells and macrophages as evaluated by single-cell RNA-sequencing (scRNA-Seq) (GSE84465). (E) Left panel: Dot plot representation of the most expressed M1 and M2 classical markers in $TLR4^+$ and $TLR4^-$ macrophages isolated from the GBM tumor core as evaluated by scRNA-Seq (GSE84465). Right panel: Control analysis showing upregulationof M1, M2 and TAM signature expression in GB tumor core macrophages *versus* astrocytes and neoplastic cell populations from scRNA-Seq. #different from NT, &different from ODG, *different from AST or at indicated comparisons (Kruskal-Wallis *post hoc* Dunn's; $p < 0.05$; In "A" Empirical Bayes Statistics was also employed).

lower expression of TLR4 when compared to AST tumors in the three datasets evaluated (Fig. 1A). Darmanis et al. reported that CD45^{+} cells within GB tumors consist of ~69% macrophages and only ~31% microglial cells [22]. Conversely, expression of macrophage (and microglia) surface marker CD14 is higher in GB and AST tumors in comparison with both the less aggressive tumor ODG and NT samples [42,43]. These patterns were consistent across two out of the three datasets evaluated (Fig. 1A). We next evaluated the expression of M1-, M2- and TAM-like signatures in glioma samples. Interestingly, M1, M2 and TAM gene signatures are enriched in GB; in AST, M1 and TAM signatures are enriched; whereas no enrichment of signatures was detected for ODG tumors in comparison with NT brain tissues (Fig. 1B). To further assess these differences, we took advantage of single-cell RNA sequencing data generated by Darmanis [22] and evaluated TLR4 mRNA expression among cell types isolated from GB tumors (Fig. 1C), as well as in myeloid/CD45^{+} cells separated into macrophage and microglia phenotypes based on gene expression signatures (Fig. 1C, heatmap). We found that TLR4 expression is higher in tumor-associated immune cells (macrophages and microglia) compared to neoplastic/GB cells (Fig. 1D), whereas oligodendrocytes, OPC and neurons showed very low/undetectable TLR4 mRNA. Interestingly, non-neoplastic astrocytes isolated from tumor periphery showed the highest levels of TLR4 mRNA (Fig. 1D), which correlates with the increased expression of TLR4 in astrocytomas *versus* more undifferentiated gliomas such as GB (Fig. 1A). Of note, the majority (90%) of GB cells are TLR4-negative, and only 42% of TAMs are TLR4-positive (log2 CPM $>$ 1), indicating that TLR4 is suppressed in a subpopulation of GB-associated macrophages (58%) (Fig. 1D, histograms). Because TLR4 is typically associated with M1-like phenotypes, we grouped tumor macrophages into TLR4-negative (log2 CPM $<$ 1) and TLR4-positive (log2 CPM $\geq$ 1) and found that both M1 and M2 markers are expressed in GB-associated macrophages (in accordance with previous data) [25]. Indeed, these gene markers showed similar patterns of expression between TLR4-negative and TLR4-positive macrophage subsets (Fig. 1E). As a control, analysis of gene signature scores confirmed that M1-, M2- and TAM-like gene sets are enriched in GB-associated macrophages when compared to other glial cell types such as astrocytes and tumor core neoplastic glial cells sequenced in single cell experiments (Fig. 1E, right graph).

3.2. Sensitive and chemoresistant glioma cells exhibit differential TLR4 expression and functionality

We next determined whether the chemoresistance phenotype impacts the expression of TLRs in glioma cells. To address this need, GL261 glioma cell resistance to TMZ was induced by exposing cell cultures to increasing concentrations of this drug [34]. We first compared cell biology characteristics of sensitive (GL) and chemoresistant (GLTMZ) gliomas in culture. GL cells exhibited the expected star-shape morphology, while GLTMZ became fusiform and elongated after the acquisition of chemoresistance (Fig. 2A-B). Interestingly, cell proliferation and viability were decreased by ~40%, 50% and 40% in GLTMZ when compared to GL cells as assessed by cell counting, BrdU and MTT assays, respectively (Fig. 2C-E). GL and GLTMZ exhibited a differential migration profile, and GL cells showed a slight migratory advantage when compared to GLTMZ following 6 and 12 h of analysis (Fig. 2F). Of note, although the GLTMZ cells exhibit lower *in vitro* proliferation rates, their implantation in an *in vivo* preclinical GB model generated larger tumors when compared to GL cells, as reported in a previous study [34].

We further investigated the TLR mRNA expression (TLR1-TLR9, TLR11-TLR13) in GL and GLTMZ cells by qPCR. Previous experiments to define the best internal control gene for absolute expression quantifications (Ppia) (Table 3S) and the primer amplification efficiency (Fig. 1S) were performed. Of note, TLR2, TLR4, TLR8 and TLR9 were expressed by GL and GLTMZ glioma cells, and no amplification signal was detected for the other TLRs described in mouse. As shown in Fig. 3 (panel A), the chemoresistance development resulted in a differential TLR expression in glioma cells, with the expression of TLR4 and TLR9 significantly downregulated (~60% and 70%, respectively) in GLTMZ when compared to GL cells. As TLR4 downregulation was observed in human GB (Fig. 1) and also described as fundamental to maintenance of GB stemness [21], the TLR4 functionality was then determined in glioma cells. We found out that TLR4 exhibits distinct pharmacological properties in GL and GLTMZ cells. The stimulation of GL cells with LPS (10 ng/mL) for 24 h induced a 60% TLR4-MD2 complex activation when compared to unstimulated cells; nonetheless, no change was observed in GLTMZ at the same experimental condition (Fig. 3B). GL and GLTMZ also exhibited a distinct migration profile in response to TLR4 agonism

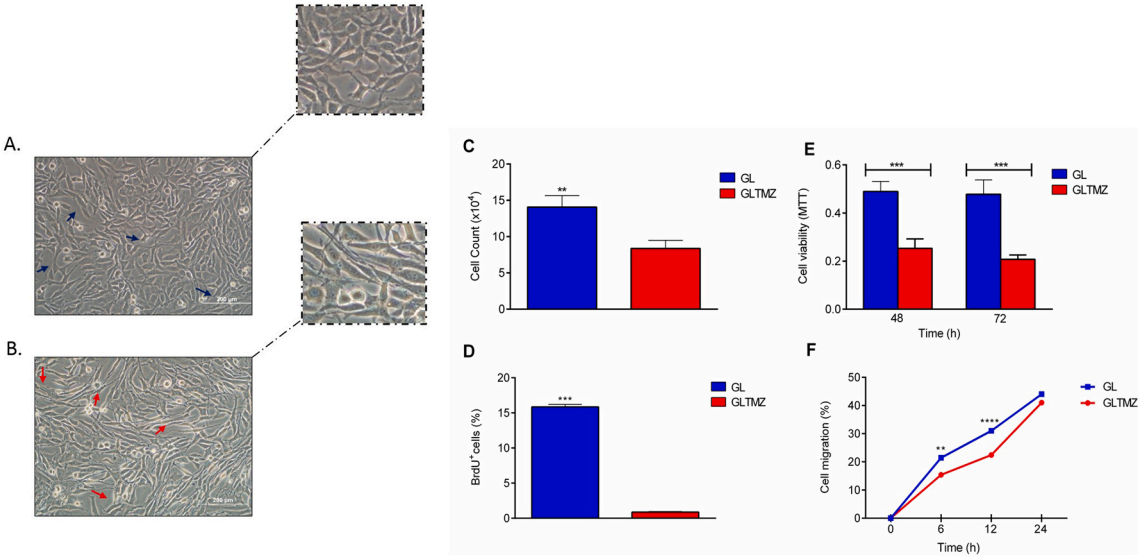

Fig. 2. Biological characteristics of sensitive and chemoresistant glioblastoma cells. The morphological differences between GL and GLTMZ are shown in (A) and (B), respectively (arrows; phase-contrast micrographs at 20× magnification). Cell proliferation analysis in GL and GLTMZ glioma cells was determined by cell counting (C), BrdU incorporation (D), MTT assay (E). GL and GLTMZ cell migration was determined by scratch-wound assay (F). Data represent the average ± standard deviation of at least two experiments performed in triplicate, analyzed by Student's *t*-test (graphs C, D and F) or ANOVA followed by Tukey's post-hoc (graph E). ** and ***Significantly different from control (GL cells; $P \leq 0.01$ and $P \leq 0.001$, respectively).
GL: GL261 glioblastoma cell sensitive to TMZ; GLTMZ: GL261 glioblastoma cell resistant to TMZ.

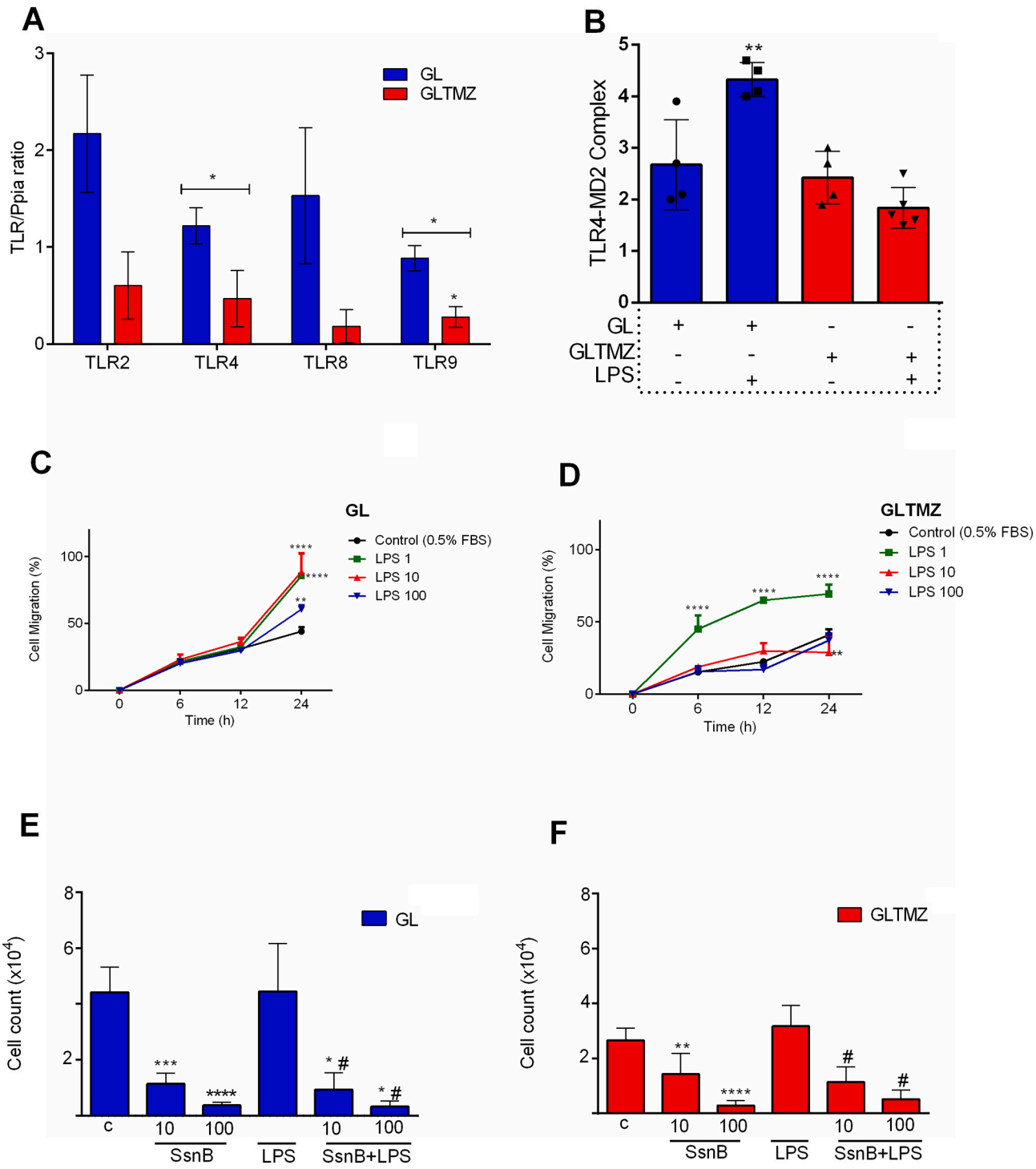

Fig. 3. Determination of TLR mRNA expression and TLR4 functionality in sensitive and chemoresistant glioblastoma cells. (A) Total mRNA of GL and GLTMZ was isolated and the mouse TLRs expression was determined by qPCR using specific primers. Data were analyzed by Student's *t*-test; *significantly different from GL cells ($P \leq 0.05$). (B) TLR4-MD2 complex activation was determined by flow cytometry in GL and GLTMZ cells following stimulation with LPS (100 ng/mL) for 18 h. Data were analyzed by Student's *t*-test. *Significantly different from control (unstimulated GL cells; $P \leq 0.05$). Glioma cell migration was determined by scratch-wound assay in GL (C) or GLTMZ (D) exposed to LPS (as indicated) for 18 h. Data were analyzed by two-way ANOVA followed by Bonferroni test. **,****Significantly different from control (unstimulated GL or GLTMZ cells; $P \leq 0.001$ and $P \leq 0.0001$, respectively). Glioma cell proliferation was determined by cell counting in GL (E) or GLTMZ (F) exposed to LPS (100 ng/mL) for 18 h in absence or in presence of SsnB (10 or 100 ng/mL), which was added to culture 30 min before LPS stimulation. Data were analyzed by one-way ANOVA followed by Tukey's post-hoc test. ***, ****Significantly different from unstimulated GL or GLTMZ cells, $P \leq 0.001$ and $P \leq 0.0001$; #significantly different from LPS stimulated GL or GLTMZ cells, $P \leq 0.0001$.

GL: GL261 glioblastoma cell sensitive to TMZ; GLTMZ: GL261 glioblastoma cell resistant to TMZ; LPS: lipopolysaccharide (TLR4 agonist); SsnB: Sparstolonin B (TLR2-TLR4 antagonist).

(Fig. 3C-D). Indeed, LPS (1, 10 and 100 ng/mL) promoted respectively 100, 100 and 50% of GL migration after 24 h of stimulation when compared to control cells (Fig. 3C). On the other hand, LPS at the lowest tested concentration (1 ng/mL) induced a sustained GLTMZ cell migration through 24 h of the experiment, while LPS at 10 ng/mL promoted a slight and biphasic effect following 12 and 24 h of analysis, and LPS at 100 ng/mL had no effect when compared to untreated cells (Fig. 3D).

In addition, the impact of LPS (100 ng/mL) on GL and GLTMZ cell proliferation was determined by cell counting in presence or absence of Sparstolonin B (SsnB), a TLR2-TLR4 selective antagonist [37]. LPS stimulation did not change the GL or GLTMZ proliferation when compared to the respective controls (Fig. 3E-F). However, the treatment with SsnB (10 and 100 μM) alone for 18 h reduced cell proliferation of GL by ~75% and 90% and of GLTMZ by ~45% and 90%, suggesting that endogenous TLR2-TLR4 stimulation maintains glioma cell survival. Of note, the treatment with LPS (100 ng/mL) did not reverse the anti-proliferative effect of SsnB. Finally, the effect of TLR4 sensitization in glioma cell proliferation, viability, and migration was also investigated by exposing the cultures to HMGB1, a DAMP and an endogenous TLR2/4 agonist [11,21]. Similarly to LPS, HMGB1 did not change cell proliferation or viability of GL and GLTMZ when compared to the control. However, the treatment impaired GLTMZ cell migration at 12 and 24 h of analysis, while no changes were detected in GL cells (Fig. 2S, A-D). These data indicate that chemoresistant cells express lower TLR4 levels and that they are more tolerant to LPS stimulation (Fig. 3B) when compared to TMZ-sensitive glioma cells, which may contribute to immune escape.

3.3. TLR4 expression and activity are downregulated in TAM

TLR4 plays a key role in the activation of innate immunity, modulating macrophage activity [45]. Therefore, since TAMs are important components for tumor progression [34,46], the impact of glioma cells on TLR4 expression and activity of macrophages was determined. Mouse and human primary macrophage cultures were obtained as described above, and co-cultured with either sensitive or chemoresistant mouse (GL; GLTMZ) or human (U87; U87TMZ) glioma cells, respectively (Fig. 4A-D). TLR4 expression was found in human macrophages as well as in macrophages co-cultured with U87 and U87TMZ, as assessed by IF staining. Interestingly, glioma cells, particularly U87TMZ, interacted with macrophages forming a cord-like structure (Fig. 4A). This characteristic has already been reported for mouse macrophage-GLTMZ co-cultures [34] and highlights the importance of macrophage-glioma crosstalk for tumor biology. Next, TLR4 mRNA expression in macrophages co-cultured with glioma cells was determined by qPCR. We found that TLR4 expression was reduced by 75% and 90% in human and mouse macrophages cultured with glioma cells, respectively, when compared to controls (human or mouse macrophages cultured alone; Fig. 4B-C). TLR4 functionality was further determined by measuring TLR4-MD2 complex in mouse macrophages cultured in presence or absence of glioma cells. The double labeling of TLR4-MD2 with CD11b was used to identify the population of macrophages that had active TLR4 and to differentiate it from active TLR4 in glioma cells (Fig. 4D). As expected, macrophages stimulated with LPS (10 ng/mL) exhibited an increase of 31% in TLR4-MD2 complex activation when compared to untreated macrophages. However, the presence of GL or GLTMZ completely impaired the TLR4-MD2 activation on macrophages even following stimulation with the TLR4 agonist (LPS), suggesting the decrease in TLR4 expression and functionality as a mechanism of glioma-induced immune escape. In line with this, increased levels of tumor-promoting cytokine IL6 (60%), immunosuppressive IL10 (180%), MCP-1 (30%) and TNF (60%) were measured in macrophages co-cultured with glioma when compared to control macrophages (Fig. 5A-D). Consistent with the lack of TLR4 response, the stimulation of macrophage-glioma co-cultures with LPS also did not change the cytokine release profile. Of note, both sensitive and chemoresistant glioma cells induced similar effects on TLR4 signaling in macrophages, indicating that TLR4 modulation in macrophages is most likely associated with glioma cell presence itself, as a fundamental mechanism of immune escape, rather than with the chemoresistance phenotype.

3.4. TLR4 and CD45 are differentially expressed in human gliomas and in metastatic brain tumors

Based on the potential immunosuppressive function of $TLR4^{low}$ macrophages in the GB tumor environment, the expression of TLR4 and CD45, a marker of hematopoietic cells also expressed by macrophages [47], was subsequently analyzed in ten brain tumor samples from patients to determine whether the prevalence of these markers may correlate with tumor aggressiveness. A cohort of 10 biopsies from patients diagnosed with primary II-IV glioma grades, IV glioma grade relapse, and brain metastatic tumors (adenocarcinoma and esophageal) undergoing treatment in ISCMPA were enrolled in this study (Fig. 3S). Interestingly, TLR4 exhibited both cytoplasmic and an uncommon nuclear staining patterns (Table 1) and its differential expression was found in the tumors analyzed (Fig. 6A-B, Fig. Supplementary Figure 4). TLR4 expression was inversely proportional to CD45, and primary IV grade glioma exhibited decreased TLR4 expression when compared to CD45, which is in accordance with TLR4 downregulation determined in GB cells, as well as in TAM evaluated by scRNA sequencing. On the other hand, higher TLR4 expression when compared to CD45 was detected in metastatic brain tumors, suggesting that the tumor origin or the metastasis process impacts TLR4 expression. The evaluation of histoscores for TLR4 and CD45 in brain tumors is summarized in Table 1.

4. Discussion

In our study, we provided evidence for the participation of TLR signaling in the modulation of TME. We identified that TLR4 expression in GB tumors (tumor bulk transcriptome) was similar to that observed in NT tissues, but lower when compared to AST tumors. Further, using reverse translational investigation, we confirmed that TLR4 expression and function are impaired in a subset of chemoresistant glioma as well as in macrophages co-cultured with GB cells. Finally, experiments performed in a cohort of clinical primary and metastatic brain tumors indicated that the TLR4 and CD45 immunostaining are inversely proportional and confirmed the low TLR4 expression in GB. Overall, our data suggest the downregulation of TLR4 expression and activity as a strategy of GB-associated immune escape.

Although multiple immune checkpoints have been described [48] and patients diagnosed with specific types of cancer have benefited from immunotherapy [49,50], the treatment of GB remains a challenge [3]. The chemoresistance development and the complexity of GB-tumor microenvironment constitute major issues for the success of therapy. GB is characterized by the induction of both local and systemic immunosuppression [51]. Multiple cell pathways are involved in the control of immune/inflammatory response in the tumor microenvironment, which is a determinant of chemotherapy response [52]. Considering the complexity and dynamical behavior of TLR signaling in the tumor context, we hypothesized that TLR4 is differentially expressed and activated in the transformed and non-transformed cell populations that compose TME, resulting in distinct biological outcomes. Therefore, here we investigated the participation of TLRs, particularly TLR4, in the scenario of cancer-related inflammation by evaluating TLR4 signaling in GB cells, TAMs, and in clinical brain tumor biopsies.

To understand the participation of TLR4 in GB-associated immune evasion, we firstly evaluated gene expression data from gliomas of 3 independent microarray datasets. The results showed that TLR4 expression is lower in GB when compared to AST. On the other hand, both GB and AST were shown to be enriched for CD14 expression when compared to NT tissues. Data from scRNA-sequencing indicated that

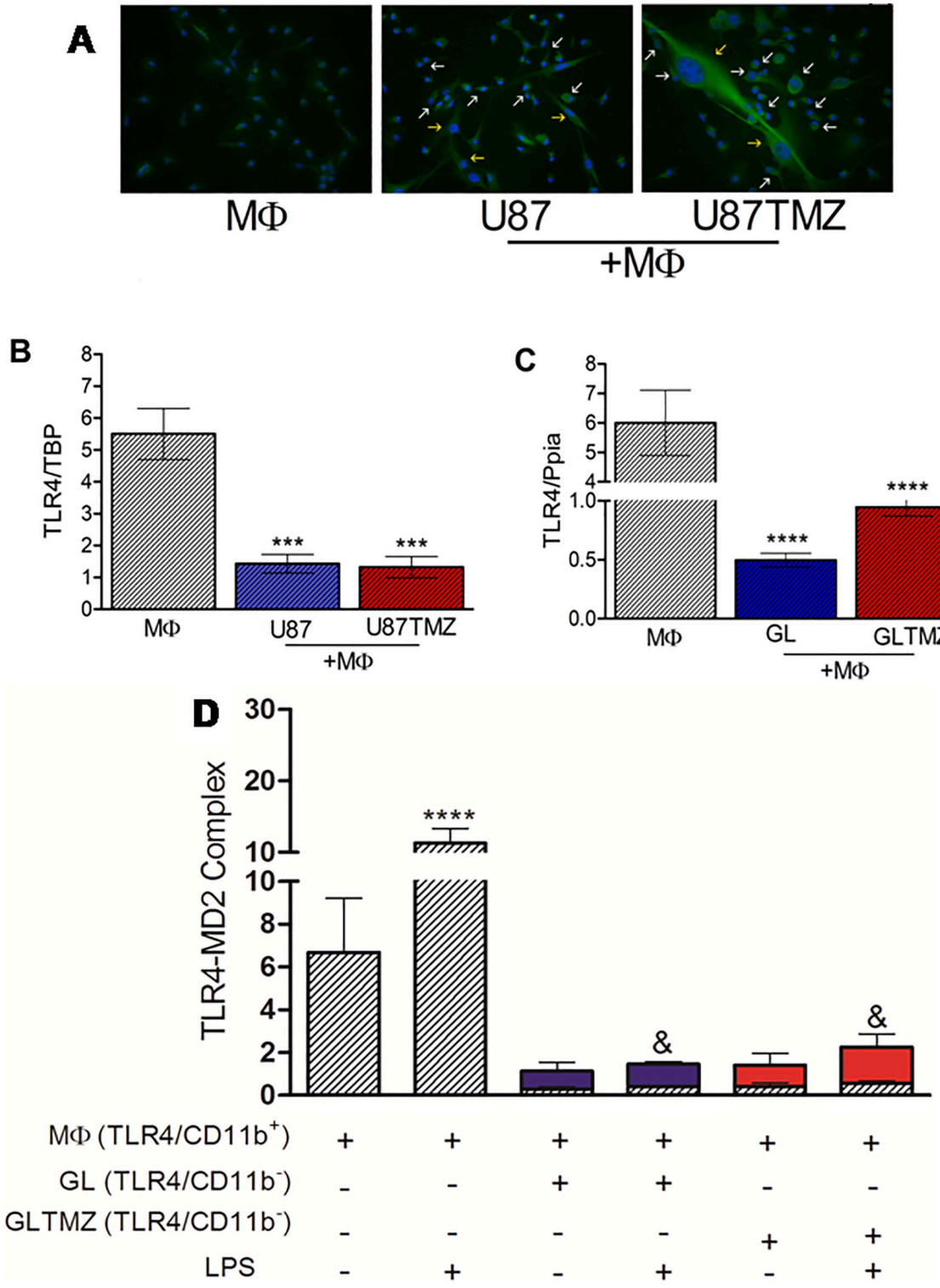

Fig. 4. Evaluation of TLR4 expression and functionality in primary macrophages co-cultured with sensitive or chemoresistant glioblastoma cells. (A) Representative images of TLR4 staining in human macrophages cultured alone or in presence of U87 or U87TMZ glioma cells determined by IF using anti-TLR4 antibody and DAPI as nucleus staining (Olympus microscope; 40× magnification; yellow arrows point glioma cells, white arrows point human macrophages). Total mRNA of human (B) or mouse (C) macrophages cultured alone or in presence of U87/U87TMZ or GL/GLTMZ, respectively, was isolated and TLR4 expression was determined by qPCR using specific primers. Data represent the average of TLR4 expression ± standard deviation of at least five samples performed in duplicate, and were analyzed by one-way ANOVA followed by Tukey's *post-hoc*.***, **** Significantly different from control (human or mouse macrophages, $P \leq 0.0002$ and $P \leq 0.0001$, respectively). (D) TLR4-MD2 complex activation was determined by flow cytometry in macrophages cultured alone, and co-cultured with either GL or GLTMZ cells in presence or absence of LPS stimulation (10 ng/mL for 18 h). Double labeling with CD11b was used to identify macrophage population. Data were analyzed by two-way ANOVA followed by Bonferroni test. ****,$^{\&}$Significantly different from controls (macrophages and macrophages stimulated with LPS, $P \leq 0.0001$).
GL: GL261 glioblastoma cell sensitive to TMZ; GLTMZ: GL261 glioblastoma cell resistant to TMZ; U87: human U87MG glioblastoma cell sensitive to TMZ; U87TMZ: human U87MG glioblastoma cell resistant to TMZ; MΦ: macrophages; LPS: lipopolysaccharide (TLR4 agonist).

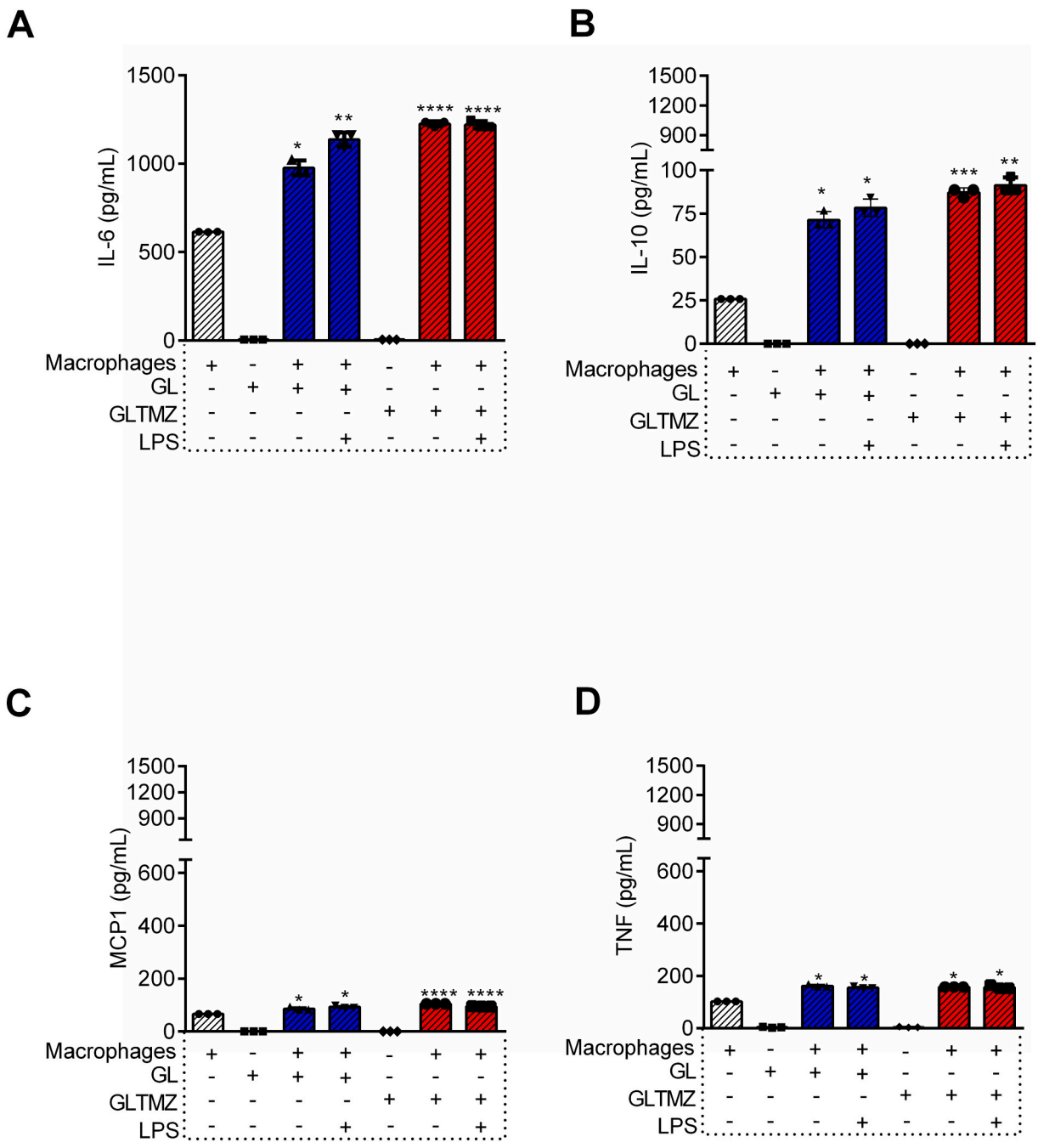

Fig. 5. Determination of cytokines production in primary mouse macrophages co-cultured with sensitive or chemoresistant glioblastoma cells. The measurement of cytokines was performed in the supernatant of macrophages cultured alone, or co-cultured with either GL or GLTMZ in presence or absence of LPS stimulation (10 ng/mL for 18 h) by flow cytometry using the CBA assay. IL-6 (A), IL-10 (B), MCP-1 (C) and TNF (D). Data represent the average ± standard deviation of at least three experiments performed in duplicate, which were analyzed by one-way ANOVA followed by Tukey's *post-hoc* test. *, **, ***, **** Significantly different from control (macrophages cultured alone, $P \leq 0.01$, $P \leq 0.0012$, $P \leq 0.0004$ and $P \leq 0.0001$, respectively). GL: GL261 glioblastoma cell sensitive to TMZ; GLTMZ: GL261 glioblastoma cell resistant to TMZ; LPS: lipopolysaccharide (TLR4 agonist).

most of the TLR4 expression occurs in myeloid/immune cells present in GB tumors, while neoplastic cells are mostly TLR4-negative. In addition, a significant subpopulation of GB-associated macrophages (58%) did not express detectable TLR4. Based on these results, we hypothesized that GB neoplastic cells could be suppressing TLR4 expression in macrophages that infiltrate GB tumors. In line with this, deeper investigations performed in GB cultures reveals that the chemoresistant cells displayed characteristics of immune escape as evidenced by the downregulation of TLR4 expression and function, even following stimulation with the agonist LPS. Indeed, cancer stem cells are described as responsible for chemoresistance phenotype and the key role of TLR4 downregulation to stemness maintenance was previously reported [21]. Considering the high cellular heterogeneity of GBs, the presence of GB-TLR4^{high} and GB-TLR4^{low} subsets in the TME and its differential activation by DAMPs may impact the composition of TME and the chemotherapy response profile.

TLR4 signaling was further investigated in macrophages-GB co-cultures, which was applied as a strategy to mimic macrophage-tumor crosstalk. Notably, TLR4 expression was lower in macrophages co-cultured with GB cells when compared to control. TLR4 functionality was also specifically impaired in macrophages and it remained

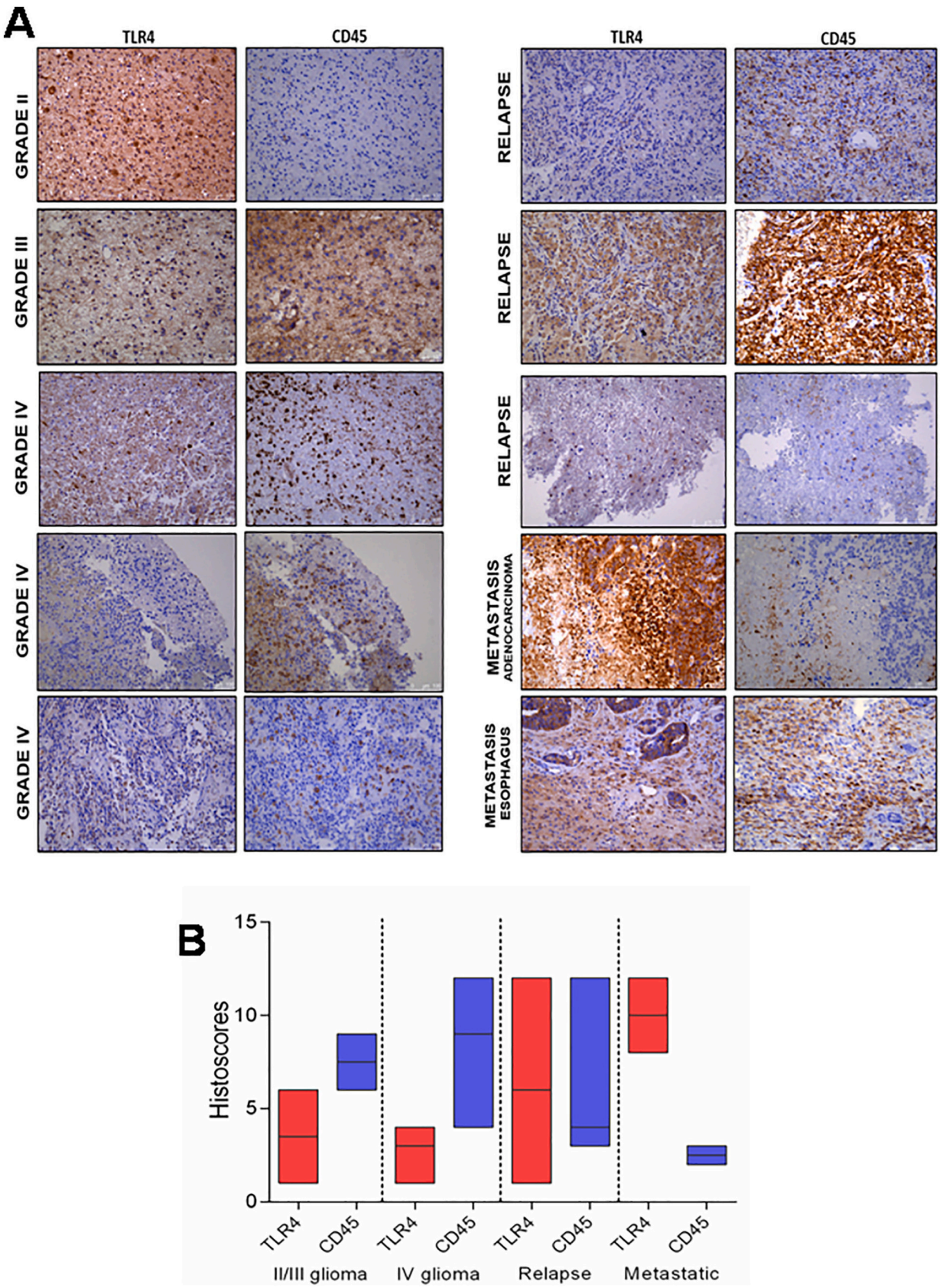

Fig. 6. Analysis of TLR4 and CD45 expression in human brain tumor biopsies. In (A) representative images of TLR4 and CD45 staining in grade II, III and IV gliomas, relapse glioma and metastatic brain tumors (as indicated) determined by IHC using anti-TLR4 and anti-CD45 antibodies in serial slices of tumor samples (DM6B optical microscope, Leica Optical, 20× magnification). (B) Through the use of the final histoscore (staining intensity and percentage of stained cells - Table 1), a graph containing the results of TLR4 and CD45 expression was constructed. Note the low TLR4 expression in grade IV glioma and the higher TLR4 expression in brain metastatic tumor, which was inversely proportional to CD45 expression.

Table 1
Evaluation of TLR4 and CD45 labeling in human brain tumors.

Sex	Age	Grade	TLR4				CD45			
			Staining intensity	Labeled cells (%)	Final score	Staining location	Staining intensity	Labeled cells (%)	Final score	Staining location
M	47	II glioma	2	3	6	Cytoplasmic and nuclear staining	3	3	9	Cytoplasmic staining
M	63	III glioma	1	1	1	Cytoplasmic staining	3	2	6	Cytoplasmic staining
M	53	IV glioma	2	2	4	Cytoplasmic and nuclear staining	2	2	4	Cytoplasmic staining
M	63	IV glioma	1	3	3	Cytoplasmic and nuclear staining	3	4	12	Cytoplasmic staining
F	46	IV glioma	1	1	1	Predominance of nuclear staining	3	3	9	Cytoplasmic staining
F	61	Relapse GB	2	3	6	Cytoplasmic staining	3	4	12	Cytoplasmic staining
F	64	Relapse GB	1	1	1	Cytoplasmic staining	2	2	4	Cytoplasmic staining
M	57	Relapse GB	3	4	12	Cytoplasmic and nuclear staining	3	1	3	Cytoplasmic staining
M	57	Metastasis (adenocarcinoma)	3	4	12	Cytoplasmic and nuclear staining	3	1	3	Cytoplasmic staining
M	73	Metastasis (esophagus)	2	4	8	Cytoplasmic and nuclear staining	2	1	2	Cytoplasmic staining

Expression of TLR4 and CD45 in biopsies of primary and metastatic brain tumors were analyzed by immunohistochemistry. TLR4 and CD45 intensities and the percentage of staining were determined by a pathologist in a blinded manner. The final score was obtained by the multiplication of intensity and the percentage of staining values.
Scores of intensity of immunostaining (0: absent; 1: light; 2: moderate; 3: intense).
Score of percentage of cell staining (0: absent; 1: up to 25%; 2: 26 to 50%; 3: 51 to 75%; 4: 76 to 100%).

unchanged even following LPS stimulation, as evidenced by the lack of both TLR4-MD2 complex activation and TNF production. In addition, the repertory of cytokines secreted in macrophage-glioma is consistent with a tumor-promoting microenvironment, containing increased levels of IL-6 and IL-10,which are important mediators of tumor migration and immune evasion, respectively [53,54]. These data are in accordance with the theory that macrophages are educated by tumor cells to develop protumor actions [46] and suggest that GB cells, regardless of their chemoresistance status, can suppress TLR4 signaling in TAMs as a mechanism of immune escape. Indeed, TLR4 stimulation is an important signal to induce the phagocytic functions of macrophages [45], and thereby its impairment may contribute to tumor immune escape.

Finally, the expression of TLR4 and CD45 was analyzed in human brain tumors. Our data demonstrate that TLR4 and CD45 are inversely expressed in gliomas, in recurrent GB and in metastatic brain tumors. In line with previous data, GB exhibited low TLR4 expression when compared to II-III grade gliomas, which was followed by increased hematopoietic-derived immune cells, as indicated by CD45 expression. In contrast to physiological conditions, in which TLR4 is located mainly on the cell surface, here the pattern of TLR4 staining was predominantly cytoplasmic and in some tumors, nuclear. Studies have shown that both TLR4 and its endogenous ligand, HMGB1, are overexpressed and become cytoplasmic during the transformation toward dysplasia [12,55,56]. The investigations suggest that the abnormal and constitutive intracellular TLR4 activation results in a chronic inflammatory process which induces immune tolerance and carcinogenesis [12]. Nonetheless, the role of nuclear and cytoplasmic TLR4 in the inflammatory response is unclear and needs to be investigated.

In conclusion, we found that TLR4 expression and functionality is impaired in chemoresistant GB cells and in TAMs. Additionally, low and cytoplasmic/nuclear TLR4 expression was detected in clinical samples of GB. Our data provide insights about the complexity of TLR signaling in GB and suggest that the differential TLR4 expression and activity in mature cancer, CSCs and TAMs is dynamic through carcinogenesis progression and could represent a mechanism of tumor immune escape. Further investigations are needed to better characterize TLR4 signaling in transformed and non-transformed cells in clinical biopsies of human GB to improve the benefits of immunotherapy based on TLR signaling.

Supplementary data to this article can be found online at https://doi.org/10.1016/j.bbadis.2021.166155.

CRediT authorship contribution statement

Conceptualization: Braganhol E., Zanotto-Filho A.

Methodology and Investigation (*in silico* experiments): Falchetti M., Zanotto-Filho A.

Methodology and Investigation (pre-clinical experiments): da Cruz L.L.P., de Souza P.O., Dal Prá M., Azambuja J.H., Bertoni A.P.S., Paz A.H.R., Araújo A.B., Fazolo T., M.R. Wink.

Methodology and Investigation (clinical experiments): de Abreu A.M., da Silva G.G., Worm P.V., de Souza P.O., Visioli F.

Funding Acquisition: E. Braganhol.

Writing-Original draft: da Cruz L.L.P.

Writing – Review & Editing: E. Braganhol, M.R. Wink, Zanotto-Filho A.

Supervision: E. Braganhol.

Declaration of competing interest

The authors declare that they have no known competing financial interests or personal relationships that could have appeared to influence the work reported in this paper.

Acknowledgements

This study was supported by the Brazilian agencies: Conselho Nacional de Desenvolvimento Científico e Tecnológico (CNPq – Processo 312187/2018-1; 422298/2016-6); Coordenação de Aperfeiçoamento de Pessoal de Nível Superior (CAPES; Código de Processamento 001); Fundação de Amparo à Pesquisa do Estado do Rio Grande do Sul (FAPERGS – Processo 19/2551-0000663-2; 19/2551-0001779-0; PRONEX - Processo 16/2551-0000473-0); Hospital de Clínicas de Porto Alegre (FIPE - Processo 2019-0059). da Cruz L.L.P., de Souza P.O., Dal Prá M., Azambuja J.H., Bertoni A.P.S., and Falchetti M. were recipients

of UFCSPA, CAPES or CNPq scholarships. Zanotto-Filho A. was recipient of Research Scholar Fellowship (CNPq-PQ2 –Processo 310665/2017-5).

References

[1] Huse, Jason T.; Holland, Eric C. Targeting brain cancer: advances in themolecular pathology of malignant glioma and medulloblastoma. Nat. Rev. Cancer, v. 10, n. 5, p. 319–331, 2010. doi:https://doi.org/10.1038/nrc2818.

[2] Che, Fengyuan et al. TLR4 interaction with LPS in glioma CD133+ cancer stem cells induces cell proliferation, resistance to chemotherapy and evasion from cytotoxic T lymphocyte-induced cytolysis. Oncotarget, v. 8, n. 32, p. 53495, 2017. doi:10.18632/oncotarget.18586.

[3] Phillips, Heidi S. et al. Molecular subclasses of high-grade glioma predict prognosis, delineate a pattern of disease progression, and resemble stages in neurogenesis. Cancer Cell, v. 9, n. 3, p. 157–173, 2006. doi:https://doi.org/10.1016/j.ccr.2006.02.019.

[4] Bartek, Jiri et al. Key concepts in glioblastoma therapy. J. Neurol. Neurosurg. Psychiatry, v. 83, n. 7, p. 753–760, 2012. doi:https://doi.org/10.1136/jnnp-2011-300709.

[5] Perazzoli, Gloria et al. Temozolomide resistance in glioblastoma cell lines: implication of MGMT, MMR, P-glycoprotein and CD133 expression. PLoS One, v. 10, n. 10, p. e0140131, 2015. doi:https://doi.org/10.1371/journal.pone.0140131.

[6] Watters, Jyoti J.; Schartner, Jill M.; Badie, Behnam. Microglia function in brain tumors. J. Neurosci. Res., v. 81, n. 3, p. 447–455, 2005. doi:https://doi.org/10.1002/jnr.20485.

[7] Lau, Eunice Yuen-Ting; Ho, Nicole Pui-Yu; Lee, Terence Kin-Wah. Cancer stem cells and their microenvironment: biology and therapeutic implications. Stem Cells Int., v. 2017, 2017. doi:https://doi.org/10.1155/2017/3714190.

[8] Chen, R. et al. Cancers take their Toll—the function and regulation of Toll-like receptors in cancer cells. Oncogene, v. 27, n. 2, p. 225–233, 2008. doi:https://doi.org/10.1038/sj.onc.1210907.

[9] Botos, Istvan; Segal, David M.; Davies, David R. The structural biology of Toll-like receptors. Structure, v. 19, n. 4, p. 447–459, 2011. doi:https://doi.org/10.1016/j.str.2011.02.004.

[10] Urban-Wojciuk, Zuzanna et al. The role of TLRs in anti-cancer immunity and tumor rejection. Front. Immunol., v. 10, p. 2388, 2019. doi:https://doi.org/10.3389/fimmu.2019.02388.

[11] Hernandez, Celine; Huebener, Peter; Schwabe, Robert F. Damage-associated molecular patterns in cancer: a double-edged sword. Oncogene, v. 35, n. 46, p. 5931–5941, 2016. doi:https://doi.org/10.1038/onc.2016.104.

[12] Jouhi, Lauri et al. Different toll-like receptor expression patterns in progression toward cancer. Front. Immunol., v. 5, p. 638, 2014. doi:https://doi.org/10.3389/fimmu.2014.00638.

[13] Vinnakota, Katyayni et al. Toll-like receptor 2 mediates microglia/brain macrophage MT1-MMP expression and glioma expansion. Neuro-oncology, v. 15, n. 11, p. 1457–1468, 2013. doi:https://doi.org/10.1093/neuonc/not115.

[14] Jin, Bo et al. The effects of TLR activation on T-cell development and differentiation. Clin. Dev. Immunol., v. 2012, 2012. doi:https://doi.org/10.1155/2012/836485.

[15] Cen, Xiaohong; Liu, Shuwen; Cheng, Kui. The role of toll-like receptor in inflammation and tumor immunity. Front. Pharmacol., v. 9, p. 878, 2018. doi:https://doi.org/10.3389/fphar.2018.00878.

[16] Pradere, Jean-Philippe; Dapito, Dianne H.; Schwabe, Robert F. The Yin and Yang of Toll-like receptors in cancer. Oncogene, v. 33, n. 27, p. 3485–3495, 2014. doi:https://doi.org/10.1038/onc.2013.302.

[17] Carpentier, Alexandre et al. Intracerebral administration of CpG oligonucleotide for patients with recurrent glioblastoma: a phase II study. Neuro-oncology, v. 12, n. 4, p. 401–408, 2010. doi:https://doi.org/10.1093/neuonc/nop047.

[18] Weigel, Brenda J. et al. Prolonged subcutaneous administration of 852A, a novel systemic toll-like receptor 7 agonist, to activate innate immune responses in patients with advanced hematologic malignancies. Am. J. Hematol., v. 87, n. 10, p. 953–956, 2012. doi:https://doi.org/10.1002/ajh.23280.

[19] Fernandez, E. et al. NfκB activation in differentiating glioblastoma stem-like cells is promoted by hyaluronic acid signaling through TLR4. Sci. Rep., v. 8, n. 1, p. 6341, 2018. doi:https://doi.org/10.1038/s41598-018-24444-6.

[20] Shi, S. et al. Expression profile of Toll-like receptors in human breast cancer. Mol. Med. Rep., v. 21, n. 2, p. 786–794, 2020. doi:https://doi.org/10.3892/mmr.2019.10853.

[21] Alvarado, A. et al. Glioblastoma cancer stem cells evade innate immune suppression of self-renewal through reduced TLR4 expression. Cell Stem Cell, 2017. doi:https://doi.org/10.1016/j.stem.2016.12.001.

[22] Darmanis, Spyros et al. Single-cell RNA-seq analysis of infiltrating neoplastic cells at the migrating front of human glioblastoma. Cell Rep., v. 21, n. 5, p. 1399–1410, 2017. doi:https://doi.org/10.1016/j.celrep.2017.10.030.

[23] Haage, Verena et al. Comprehensive gene expression meta-analysis identifies signature genes that distinguish microglia from peripheral monocytes/macrophages in health and glioma. Actaneuropathologica Commun., v. 7, n. 1, p. 1–18, 2019. doi:https://doi.org/10.1186/s40478-019-0665-y.

[24] Kennedy, Benjamin C. et al. Tumor-associated macrophages in glioma: friend or foe?. J. Oncol., v. 2013, 2013. doi:https://doi.org/10.1155/2013/486912.

[25] Müller, Sören et al. Single-cell profiling of human gliomas reveals macrophage ontogeny as a basis for regional differences in macrophageactivation in the tumor microenvironment. Genome Biol., v. 18, n. 1, p. 234, 2017. doi:https://doi.org/10.1186/s13059-017-1362-4.

[26] Vasiliadou, Ifigenia; Holen, Ingunn. The role of macrophages in bone metastasis. J. Bone Oncol., v. 2, n. 4, p. 158–166, 2013. doi:https://doi.org/10.1016/j.jbo.2013.07.002.

[27] Murray, Peter J. et al. Macrophage activation and polarization: nomenclature and experimental guidelines. Immunity, v. 41, n. 1, p. 14–20, 2014. doi:https://doi.org/10.1016/j.immuni.2014.06.008.

[28] Jayasingam, Sharmilla Devi et al. Evaluating the polarization of tumor-associated macrophages into M1 and M2 phenotypes in human cancer tissue: technicalities and challenges in routine clinical practice. Front. Oncol., v. 9, 2019. doi:https://doi.org/10.3389/fonc.2019.01512.

[29] Rogers, Thea L.; Holen, Ingunn. Tumour macrophages as potential targets of bisphosphonates. J. Transl. Med., v. 9, n. 1, p. 177, 2011. doi:https://doi.org/10.1186/1479-5876-9-177.

[30] Zhu, Changbin et al. The contribution of tumor-associated macrophages in glioma neo-angiogenesis and implications for anti-angiogenic strategies. Neuro-oncology, v. 19, n. 11, p. 1435–1446, 2017. doi:https://doi.org/10.1093/neuonc/nox081.

[31] Takeya, Motohiro; Komohara, Yoshihiro. Role of tumor-associated macrophages in human malignancies: friend or foe?. Pathol. Int., v. 66, n. 9, p. 491–505, 2016. doi:https://doi.org/10.1111/pin.12440.

[32] Ebi, Hiromichi et al. Relationship of deregulated signaling converging onto mTOR with prognosis and classification of lung adenocarcinoma shown by two independent in silico analyses. Cancer Res., v. 69, n. 9, p. 4027–4035, 2009. doi:https://doi.org/10.1158/0008-5472.CAN-08-3403.

[33] Oliva, C.R. et al. Acquisition of chemoresistance in gliomas is associated with increased mitochondrial coupling and decreased ros production. J. Biol. Chem. v285, p39759–39767, 2010. doi:https://doi.org/10.1371/journal.pone.0024665.

[34] Azambuja, J. et al. Glioma sensitive or chemoresistant to temozolomide differentially modulate macrophage protumor activities. BBA-Gen. Subjects 2017. doi:https://doi.org/10.1016/j.bbagen.2017.07.007.

[35] M. Parisi, et al., Standardization of Monocyte Purification Technique as a Cell Culture Model for the Study of Macrophage Differentiation *In Vitro*, Universidade Federal do Rio Grande do Sul, 2014 (Dissertation).

[36] Menck, K. et al. Isolation of human monocytes by double gradient centrifugation and their differentiation to macrophages in teflon-coated cell culture bags. J. Vis. Exp., n. 91, p. e51554, 2014. doi:https://doi.org/10.3791/51554.

[37] Liang, Q. et al. Characterization of sparstolonin B, a Chinese herb-derived compound, as a selective Toll-like receptor antagonist with potent anti-inflammatory properties. J. Biol. Chem., v. 286, n. 30, p. 26470–26479, 2011. doi:https://doi.org/10.1074/jbc.M111.227934.

[38] Azambuja, J. et al. Inhibition of the adenosinergic pathway in cancer rejuvenates innate and adaptive immunity. Int. J. Mol. Sci., v. 20, n. 22, p. 5698, 2019. doi:https://doi.org/10.3390/ijms20225698.

[39] Pedra, Nathalia Stark et al. Endophytic fungus isolated fromachyroclinesatureioides exhibits selective antiglioma activity—the role of Sch-642305. Front. Oncol., v. 8, p. 476, 2018. doi:https://doi.org/10.3389/fonc.2018.00476.

[40] Aithal, M. et al. Validation of housekeeping genes for gene expression analysis in glioblastoma using quantitative real-time polymerase chain reaction. Brain Tumor Res. Treat., v. 3, n. 1, p. 24–29, 2015. doi:10.14791/btrt.2015.3.1.24.

[41] Vandesompele, Jo et al. Accurate normalization of real-time quantitative RT-PCR data by geometric averaging of multiple internal control genes. Genome Biol., v. 3, n. 7, p. research0034.1, 2002. doi:https://doi.org/10.1186/gb-2002-3-7-research0034.

[42] Deininger, Martin H.; Meyermann, Richard; Schluesener, Hermann J. Expression and release of CD14 in astrocytic brain tumors. Actaneuropathologica, v. 106, n. 3, p. 271–277, 2003. doi:https://doi.org/10.1007/s00401-003-0727-9.

[43] Prosniak, Michael et al. Glioma grade is associated with the accumulation and activity of cells bearing M2 monocyte markers. Clin. Cancer Res., v. 19, n. 14, p. 3776–3786, 2013. doi:https://doi.org/10.1158/1078-0432.CCR-12-1940.

[45] Hume, D. et al. The many alternative faces of macrophage activation. Front. Immunol. v. 6, p. 370, 2015. doi:https://doi.org/10.3389/fimmu.2015.00370.

[46] Mantovani, A. et al. Tumour associated macrophages as treatment targets in oncology. Nat. Rev. Clin. Oncol., v. 14 n.7, p. 399–416, 2017. doi:https://doi.org/10.1038/nrclinonc.2016.217.

[47] Pfau, J. et al. Monoclonal antibodies to CD45 modify LPS-induced arachidonic acid metabolism in macrophages. Biochim. Biophys. Acta, Mol. Cell Res., v. 1495, n. 3, p. 212–222, 2000. doi:https://doi.org/10.1016/S0167-4889(99)00171-8.

[48] Pfannenstiel, Lukas W. et al. Immune-checkpoint blockade opposes CD8+ T-cell suppression in human and murine Cancer. Cancer Immunol. Res., v. 7, n. 3, p. 510–525, 2019. doi:https://doi.org/10.1158/2326-6066.CIR-18-0054.

[49] Sharma, Padmanee; Allison, James P. The future of immune checkpoint therapy. Science, v. 348, n. 6230, p. 56–61, 2015. doi:https://doi.org/10.1126/science.aaa8172.

[50] Sharma, Padmanee; Allison, James P. Immune checkpoint targeting in cancer therapy: toward combination strategies with curative potential. Cell, v. 161, n. 2, p. 205–214, 2015. doi:https://doi.org/10.1016/j.cell.2015.03.030.

[51] Adhikaree, Jason et al. Resistance mechanisms and barriers to successful immunotherapy for treating glioblastoma. Cells, v. 9, n. 2, p. 263, 2020. doi:https://doi.org/10.3390/cells9020263.

[52] Ramón, Y. et al. Clinical implications of intratumor heterogeneity: challenges and opportunities. J. Mol. Med., 2020. doi:https://doi.org/10.1007/s00109-020-01874-2.

[53] Lamano, J. et al. Glioblastoma-derived IL6 induces immunosuppressive peripheral myeloid cell PD-L1 and promotes tumor growth. Clin. Cancer Res., v. 25, n. 12, p. 3643–3657, 2019. doi:https://doi.org/10.1158/1078-0432.CCR-18-2402.

[54] Rolle, C. et al. Mechanisms of immune evasion by gliomas. In: Glioma. Springer, New York, NY, p. 53–76, 2012. doi:https://doi.org/10.1007/978-1-4614-3146-6_5.

[55] Castellani, P. et al. Inflammation, DAMPs, tumor development, and progression: a vicious circle orchestrated by redox signaling. Antioxid. Redox Signal., v. 20, n. 7, p. 1086–1097, 2014. doi:https://doi.org/10.1089/ars.2012.5164.

[56] Jube, S. et al. Cancer cell secretion of the DAMP protein HMGB1 supports progression in malignant mesothelioma. Cancer Res., v. 72, n. 13, p. 3290–3301, 2012. doi:https://doi.org/10.1158/0008-5472.CAN-11-3481.